ACI MATERIALS JOURNAL TECHNICAL PAPER

Title no. 108-M28

Validation of Performance-Dependent Failure Criterion for Concretes

by Paula Folino and Guillermo Etse

This paper focuses on the reformulation of the internal functions of the performance-dependent failure criterion (PDFC) for concrete, proposed by the authors, and its validation for different concrete qualities and stress states. The PDFC predicts the maximum strengths of plain concretes characterized by uniaxial compressive strengths in the range of 20 to 120 MPa (2901 to 17,405 psi). Concrete performance in this criterion is defined in terms of four material features. Supported on an extensive experimental database, they are reformulated in this work as a function of the two parameters that most effectively describe the involved concrete quality: f_c' and the so-called concrete performance parameter. The objective definition of the involved concrete quality by means of these two fundamental material parameters is also demonstrated.

The numerical validation analysis in this paper illustrates the capabilities of the PDFC—when the internal functions as described in this work are considered—to predict the maximum strength properties of concretes of different qualities. Moreover, as the experimental data considered in this analysis include biaxial and triaxial test results on concrete specimens that involve a wide spectrum of confining pressures and stress meridians, the results in this work not only demonstrate the accuracy of the PDFC dependent functions on all three stress invariants, but also their variations with the involved quality.

Keywords: biaxial strength; biaxial stress; failure criterion; high-strength concrete; normal-strength concrete; performance parameter; triaxial stress; verification analysis; water-binder ratio.

INTRODUCTION

The current development of concrete technology allows the fabrication of concretes with very high-strength properties. This development has led to an extensive use of high-strength concrete (HSC) in structural components of high responsibility. Nevertheless, there are still many unknown aspects demanding further comprehensive analysis to fully understand the failure properties and mechanics governing the response behavior of these materials. From the theoretical and numerical standpoints, the best demonstration of this need is the lack of feasible material models and, moreover, strength criteria to realistically predict concrete strength properties not only in terms of the acting stresses but also of the material quality involved.

Regarding concrete quality, currently one of the most challenging items is the identification of accurate indicators of this relevant material feature controlling the complex variations of concrete strength properties in the stress invariant space. Experimental evidence demonstrates that under increasing concrete quality (when only defined by the uniaxial compressive strength f_c'), nonhomogeneous expansion of the maximum strength surface takes place in both the meridian and deviatoric views. The best indicator of this fact is the tensile-compressive strength ratio. Instead of remaining constant, it decreases for increasing f_c'. In the case of normal-strength concrete (NSC), this ratio is approximately 10 to 15%, whereas in the case of HSC, it ranges from 5 to 8%.

Regarding the influence of the stress state on concrete maximum strength, further analysis is still required to reproduce the complex dependency on this maximum strength on the third invariant of the deviatoric stress tensor and, particularly, the variation of this dependent function with the involved concrete quality.

Most of the available three-dimensional (3-D) failure criteria in the literature[1-3] were developed for NSC, whereas only a few are related to HSC.[4,5] Although some of them are able to accurately reproduce maximum strength surfaces of NSC or HSC, severe limitations arise when their applications are extended to cover both NSC and HSC. This is due to the anisotropic evolution of the concrete maximum strength surface with the involved material quality. Such anisotropic dependence of the failure surface on the concrete quality cannot be reproduced by only updating material parameters. It requires, in addition, the identification of feasible indicators of the involved material quality and the consideration of the appropriate evolution laws of the concrete strength surface in terms of these quality indicators.

Only very few proposals of maximum strength criterion are related to both NSC and HSC. One of them is by Seow and Swaddiwudhipong,[6] which takes into account an extensive experimental database to define a normalized maximum strength criterion valid for concretes of arbitrary qualities. The resulting surface is the one that best fits the considered experimental data points. Although it is easy to implement, this maximum strength criterion[6] may lead to a considerable loss of accuracy in some cases.

A recent work by Folino et al.[7] proposes the so-called performance-dependent failure criterion (PDFC) that describes the maximum strength surfaces of concrete characterized by uniaxial compressive strengths in the range of 20 to 120 MPa (2901 to 17,405 psi). Through one single equation expressed as a function of the performance parameter f_c' and three other material features—the tensile strength, the biaxial compression strength, and a friction parameter—the PDFC is able to reproduce the inhomogeneous or nonregular variations of the concrete maximum strength surface—in both the deviatoric and meridian views—with the considered material quality.

One of the relevant features of the PDFC is the inclusion of the so-called performance parameter that, together with f_c', defines the involved concrete quality. The performance

ACI Materials Journal, V. 108, No. 3, May-June 2011.
MS No. M-2009-273.R3 received August 19, 2010, and reviewed under Institute publication policies. Copyright © 2011, American Concrete Institute. All rights reserved, including the making of copies unless permission is obtained from the copyright proprietors. Pertinent discussion including authors' closure, if any, will be published in the March-April 2012 *ACI Materials Journal* if the discussion is received by December 1, 2011.

ACI member **Paula Folino**, *Civil Engineer, is a Researcher at the University of Buenos Aires (FIUBA), Buenos Aires, Argentina. Her research interests include structural engineering, material science, computational mechanics, and constitutive modeling.*

ACI member **Guillermo Etse** *is a CONICET Senior Researcher at the University of Buenos Aires. He received his doctoral degree in engineering from Karlsruhe University, Karlsruhe, Germany. His research interests include structural engineering, computational mechanics, and constitutive modeling.*

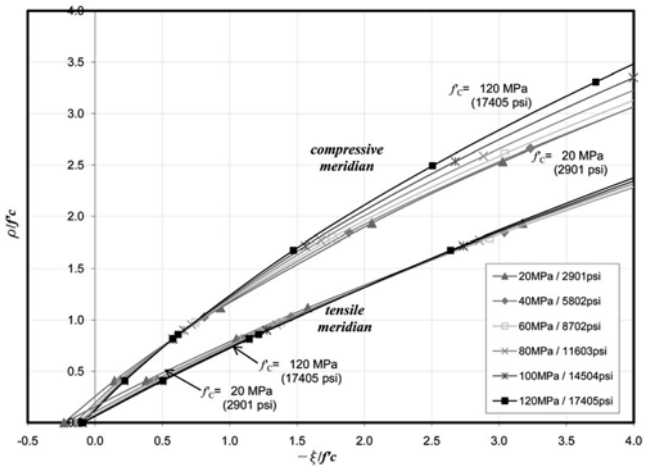

Fig. 1—Compressive and tensile meridians predicted by PDFC for different concrete qualities.

parameter is defined in terms of f_c' and the water-binder ratio (w/b) to account for the concrete porosity that strongly influences material quality.

In this work, based on an extensive experimental database extracted from the literature, the internal functions of the PDFC are reformulated to express all material parameters related to material quality in terms of both the performance parameter and f_c'. It is demonstrated that the unambiguous definition of the involved concrete quality requires the simultaneous consideration of both material parameters.

This paper also evaluates the capability of the PDFC with the internal functions as proposed in this work to reproduce the dependence of the concrete maximum strength surface on the involved concrete quality. Moreover, as experimental results of biaxial and triaxial tests that activate a wide spectrum of confining pressure and stress meridians are considered, the good agreement between the PDFC strength predictions and the experimental results demonstrates the accuracy of this failure criterion to reproduce the strong sensitivity of concrete maximum strength capacity regarding variations of all three stress invariants.

RESEARCH SIGNIFICANCE

The extensive use of HSCs demands accurate failure criteria that realistically reproduce concrete strength variation with both stress state and performance. Although the PDFC contributed to the solution of this demand, it has an intrinsic complexity, as it is expressed in terms of four material parameters. The research significance of this work is the formulation of internal functions to express all material features in terms of only two relevant parameters (f_c' and the performance parameter) that, as demonstrated herein, unambiguously define the concrete performance.

The significance of this work is also to verify the PDFC predictive capabilities when a wide spectra of stress states and material performances are considered.

PERFORMANCE-DEPENDENT FAILURE CRITERION (PDFC)

The PDFC for concretes of arbitrary strength covers the entire spectrum of concrete quality from NSC to HSC. It is represented by two quadratic parabolas for the compressive and tensile meridians with a common vertex on the hydrostatic axis in the 3-D stress space defined by the Haigh Westergaard stress coordinates. The dependence of the strength criterion on the Lode angle θ follows the elliptical function of the five parameters model by Willam and Warnke.[3]

The compressive and tensile meridians are fully defined in terms of four material parameters: the uniaxial compressive strength f_c', the uniaxial tensile strength f_t', the biaxial compressive strength f_b', and the tangent to the compressive meridian on the peak second invariant of the deviatoric stress tensor that corresponds to the uniaxial compression test (so-called m). Experimental evidence demonstrates that these parameters appropriately and objectively define the concrete quality.[7] Figure 1 illustrates the tensile and compressive meridians of concretes of different qualities according to the proposed criterion.

This criterion is valid for plain concrete with uniaxial compressive strengths f_c' in the range of 20 to 120 MPa (2901 to 17,405 psi). It appropriately reproduces the nonisotropic evolution of the concrete failure surface with increasing strength performances or quality, as may be observed by comparing Fig. 2(a) and (b).

The criterion is defined in the Haigh Westergaard stress space in terms of the normalized (with respect to f_c') stress coordinates $\bar{\xi}$ and $\bar{\rho}$, which are functions of the first and second invariant of the stress and deviatoric tensor, respectively. According to this criterion, concrete failure occurs when the normalized second Haigh Westergaard stress coordinate $\bar{\rho}$ reaches the critical normalized shear strength $\bar{\rho}^*$

$$F_{(\xi,\rho,\theta,f_c',\beta_p)} = \frac{\bar{\rho}}{\bar{\rho}^*} - 1 = 0 \tag{1}$$

In the deviatoric plane, the elliptic interpolation between the compressive and tensile meridians ρ_c and ρ_t, respectively, by Willam and Warnke[3] is followed

$$\forall \quad 0° \le \theta \le 60° \Rightarrow \bar{\rho}^* = \frac{\bar{\rho}_c}{r} \tag{2}$$

where

$$r = \frac{4(1-e^2)\cos^2\theta + (2e-1)^2}{2(1-e^2)\cos\theta + (2e-1)\sqrt{4(1-e^2)\cos^2\theta + 5e^2 - 4e}} \tag{3}$$

Thereby, θ is the Lode angle and e is the eccentricity, defined as

$$e = \frac{\bar{\rho}_t}{\bar{\rho}_c} \tag{4}$$

The parabolic equation defining the meridian traces of the PDFC results in

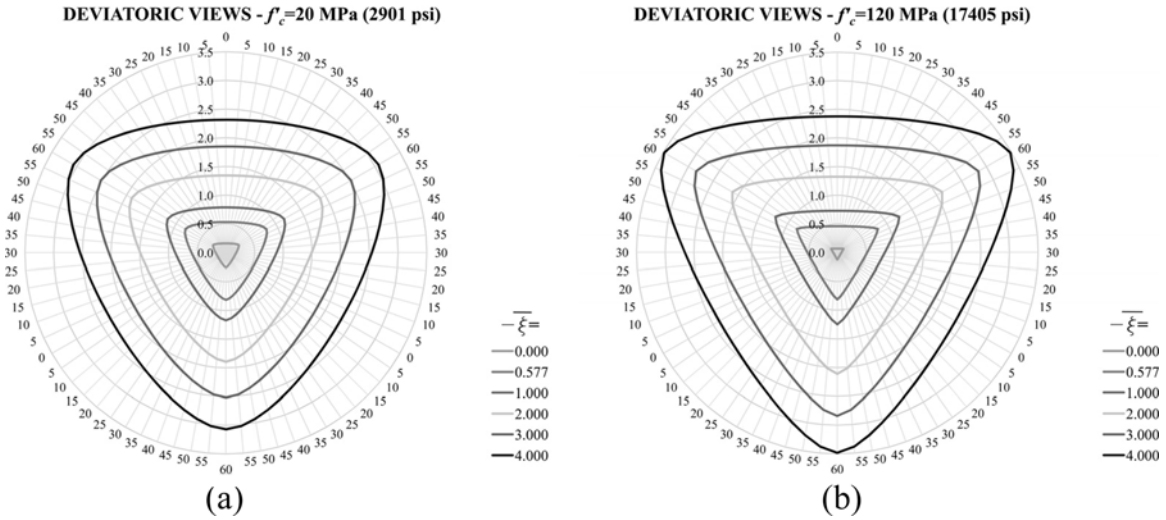

Fig. 2—Deviatoric views predicted by PDFC for extreme concrete qualities: (a) 20 MPa (2901 psi); and (b) 120 MPa (17,405 psi).

$$F = Ar^2(\bar{\rho}^*)^2 + B_c r\bar{\rho}^* + C\bar{\xi} - 1 = 0 \tag{5}$$

The compressive meridian is obtained when

$$\theta = \frac{\pi}{3} \Rightarrow A\bar{\rho}_c^2 + B_c\bar{\rho}_c + C\bar{\xi} - 1 = 0 \tag{6}$$

whereas the tensile meridian is obtained when

$$\theta = 0 \Rightarrow A\bar{\rho}_t^2 + B_t\bar{\rho}_t + C\bar{\xi} - 1 = 0 \tag{7}$$

The coefficients A, B_c, B_t, and C in Eq. (5) to (7) defining the shape of the maximum strength meridians account for the involved material performance. A basic hypothesis in the PDFC is that two normalized strengths—the uniaxial tensile $\alpha_t = f_t'/f_c'$ and the biaxial compressive $\alpha_b = f_b'/f_c'$ strengths—together with the frictional parameter m (which geometrically represents the tangent to the strength parabola on the uniaxial compressive strength point) fully define the shape of the quadratic maximum strength curves in both the tensile and compressive meridians when they are expressed in the normalized stress coordinates $\bar{\xi}$ and $\bar{\rho}$. The dependent functions of the coefficients A, B_c, B_t, and C in terms of m, α_t, and α_b are

$$A = -\frac{3}{2}\left\{1 + \frac{(m-\sqrt{2})(1-\alpha_b\alpha_t)(\alpha_b-\alpha_t)}{\alpha_b\alpha_t[(m-\sqrt{2})(\alpha_b-\alpha_t)+3m]}\right\} \tag{8}$$

$$B_c = \sqrt{3}\left\{\sqrt{2} + \frac{(\sqrt{2}m-1)(1-\alpha_b\alpha_t)(\alpha_b-\alpha_t)}{\alpha_b\alpha_t[(m-\sqrt{2})(\alpha_b-\alpha_t)+3m]}\right\} \tag{9}$$

$$B_t = \sqrt{\frac{3}{2}}\left\{\frac{1+\alpha_t^2}{\alpha_t} + \frac{[(m-\sqrt{2})\alpha_t - m](1-\alpha_b\alpha_t)(\alpha_b-\alpha_t)}{\alpha_b\alpha_t[(m-\sqrt{2})(\alpha_b-\alpha_t)+3m]}\right\} \tag{10}$$

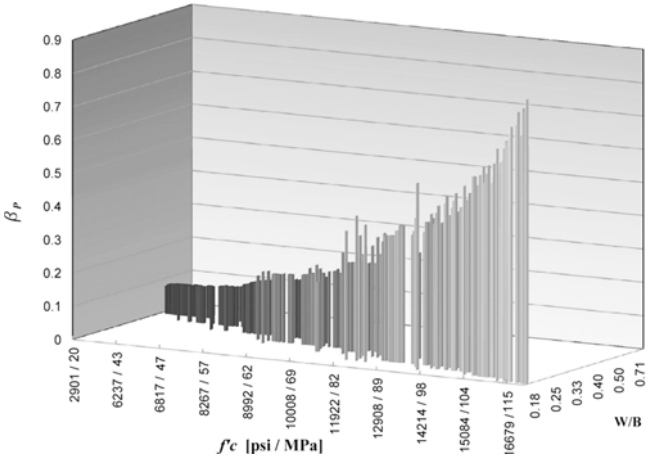

Fig. 3—Dependence of performance parameter on f_c' *and* w/b.

$$C = \sqrt{3}m\frac{(1-\alpha_b\alpha_t)(\alpha_b-\alpha_t)}{\alpha_b\alpha_t[(m-\sqrt{2})(\alpha_b-\alpha_t)+3m]} \tag{11}$$

A second relevant consideration of the PDFC is that the friction m and the normalized strengths α_t and α_b depend, in turn, on one fundamental mechanical property—f_c'—and on the most important hydrochemical feature of the cement paste—that is, w/b. These two basic parameters fully and unambiguously define the involved concrete performance through the so-called performance parameter β_P as follows

$$\begin{aligned} \beta_P &= \frac{1}{1000}\frac{f_c'}{(w/b)} \qquad f_c' \text{ in MPa} \\ \left(\beta_P &= \frac{1}{145,000}\frac{f_c'}{(w/b)}\right) \quad f_c' \text{ in psi} \end{aligned} \tag{12}$$

It varies between 0 and 1 and increases with the involved performance or quality.

The coupling between the three variables in Eq. (12)—that is, β_P, f_c', and w/b—can be clearly recognized in Fig. 3, which is based on an extensive database corresponding to the

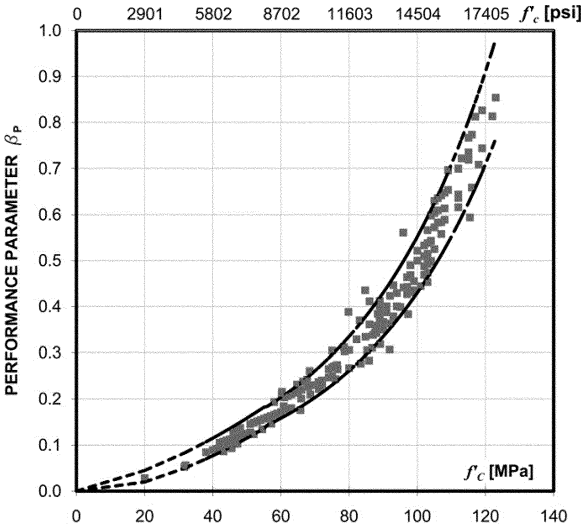

Fig. 4—Performance parameter in terms of f'_c.

experimental results of the maximum strengths of concrete specimens. To demonstrate the dependence of the performance parameter or the involved concrete quality in both *w*/*b* and f'_c, the influence of the first one is neglected. Consequently, Eq. (12) turns to $\beta_P = f'_c/1000$, and the performance parameter would only depend on f'_c. When plotting the relationship between these two, neglecting the influence of *w*/*b*, the 3-D diagram of Fig. 3 gives rise to the two-dimensional (2-D) diagram in Fig. 4. As expected, β_P cannot uniquely be defined by only f'_c. Nevertheless, as in most cases, *w*/*b* is unknown; the diagram in Fig. 4 allows the definition of the spectrum of possible β_P for each f'_c. This spectrum is bounded by the limiting curves defined as

$$\beta_{Pmax}\begin{cases}(2.60\times10^{-4})(f'_c\,[\text{MPa}]+5)^{1.60} & \\ [(9.05\times10^{-8})(f'_c\,[\text{psi}]+725)^{1.60}] & f'_c \le 55\text{ MPa (7977 psi)}\\ (4.00\times10^{-2})e^{(2.5\times10^{-2})(f'_c\,[\text{MPa}]+5)} & \\ \left[(4.00\times10^{-2})e^{(17.24\times10^{-5})(f'_c\,[\text{psi}]+725)}\right] & f'_c > 55\text{ MPa (7977 psi)}\end{cases} \tag{13}$$

$$\beta_{Pmin}\begin{cases}(2.60\times10^{-4})(f'_c\,[\text{MPa}]-5)^{1.60} & \\ [(9.05\times10^{-8})(f'_c\,[\text{psi}]-725)^{1.60}] & f'_c \le 55\text{ MPa (7977 psi)}\\ (4.00\times10^{-2})e^{(2.5\times10^{-2})(f'_c\,[\text{MPa}]-5)} & \\ [(4.00\times10^{-2})e^{(17.24\times10^{-5})(f'_c\,[\text{psi}]-725)}] & f'_c > 55\text{ MPa (7977 psi)}\end{cases} \tag{14}$$

They are expressed in terms of f'_c and are indicated by the dashed lines in Fig. 4.

Therefore, β_P can be unambiguously determined by Eq. (12); or when the *w*/*b* is unknown, it can be selected from the range of possible values defined by Eq. (13) and (14).

Once the parameters accounting for the material performance (f'_c and *w*/*b*, or simply f'_c and β_P) are determined, the most appropriate internal functions relating the material parameters (friction *m* and normalized strengths α_t and α_b) with f'_c and β_P still need to be defined. This is done in the following sections. After substituting these functions in the expressions of coefficients *A*, B_c, B_t, and *C* (Eq. (8) to (11)), the PDFC only depends on f'_c and β_P.

COUPLING OF MATERIAL PARAMETERS

The PDFC maximum strength curve in the deviatoric view is based on the elliptical description by Willam and Warnke[3] that imposes the eccentricity $e = \overline{\rho}_t/\overline{\rho}_c$ to be $0.50 \le e \le 1.00$. It may be demonstrated that this implies that the ratio between the coefficients B_c and B_t must be

$$0.50 \le B_c/B_t \le 1.00 \tag{15}$$

After replacing B_c and B_t in Eq. (15) by their expressions in Eq. (9) and (10), the related constraints between the material parameters *m*, α_t, and α_b are obtained. In other words, the elliptic form of the deviatoric views of the concrete maximum strength surface imposes a coupling between the aforementioned material parameters.

This constraint plays an important role in the calibration of the final internal functions in terms of f'_c and β_P.

INTERNAL FUNCTIONS DEPENDING ON CONCRETE PERFORMANCE

Based on several experimental results including both biaxial and triaxial test results, the internal functions relating the friction *m* and the normalized strengths α_t and α_b with f'_c and β_P are redefined as follows

$$m_{(\beta_P, f'_c)} = k_m \beta_P^{0.05}$$

$$k_m = \begin{cases}1.04 + 0.05 f'_c\,[\text{MPa}]/90 & \\ [1.04 + 0.05 f'_c\,[\text{psi}]/13,050] & f'_c < 90\text{ MPa (13,053 psi)}\\ 1.09 & f'_c \ge 90\text{ MPa (13,053 psi)}\end{cases} \tag{16}$$

$$\alpha_{t(\beta_{P,}\, f'_c)} = \frac{6.70\beta_P^{0.27}}{(f'_c\,[\text{MPa}])} \qquad \left[\alpha_{t(\beta_{P,}\, f'_c)} = \frac{972\beta_P^{0.27}}{(f'_c\,[\text{psi}])}\right] \tag{17}$$

$$\alpha_{b(\beta_{P,}\, f'_c)} = k_b\alpha_t \ge \alpha_{bmin}$$

$$k_b = 2.70(f'_c\,[\text{MPa}])^{0.45} \le 20 \qquad [k_b = 0.29(f'_c\,[\text{psi}])^{0.45} \le 20] \tag{18}$$

In Eq. (18), α_{bmin} represents the minimum possible α_b to satisfy the constraint in Eq. (15).

PDFC IN BIAXIAL STRESS SPACE

In this paper, the calibration and evaluation of the predictive capabilities of the PDFC include the consideration of concrete specimens subjected to biaxial stress states. Therefore, it is relevant to analyze the plots of the PDFC maximum strength surface in this particular stress state.

Departing from known material parameters f'_c and β_P and based on evaluations of coefficients *A*, B_c, B_t, and *C* by means of the internal functions Eq. (16) to (18), the surface of the PDFC for the involved concrete performance can be fully determined.

Figures 5(a) and (b) illustrate biaxial plots of the PDFC corresponding to defined qualities β_P and f'_c. As can be observed, surface curvatures in the compression-compression quadrant decrease for increasing f'_c, while remaining

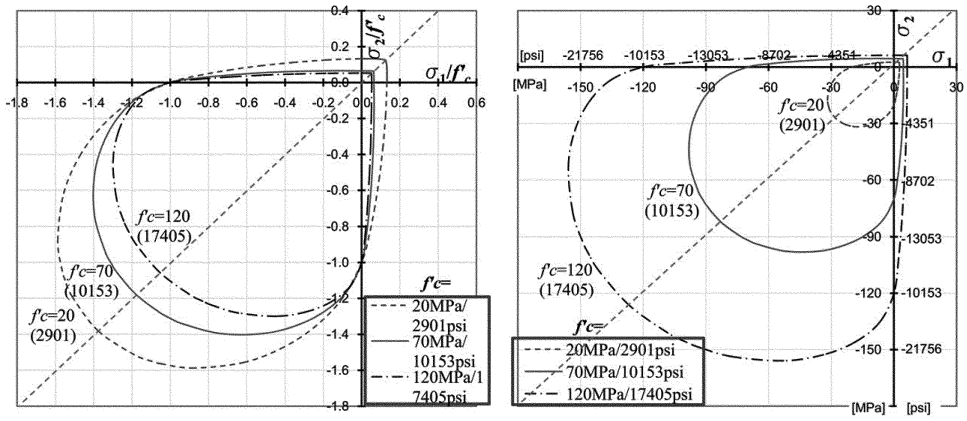

(a) (b)

Fig. 5—Biaxial failure curves predicted for different f_c' *and* β_P *medium values: (a) normalized plot; and (b) non-normalized plot.*

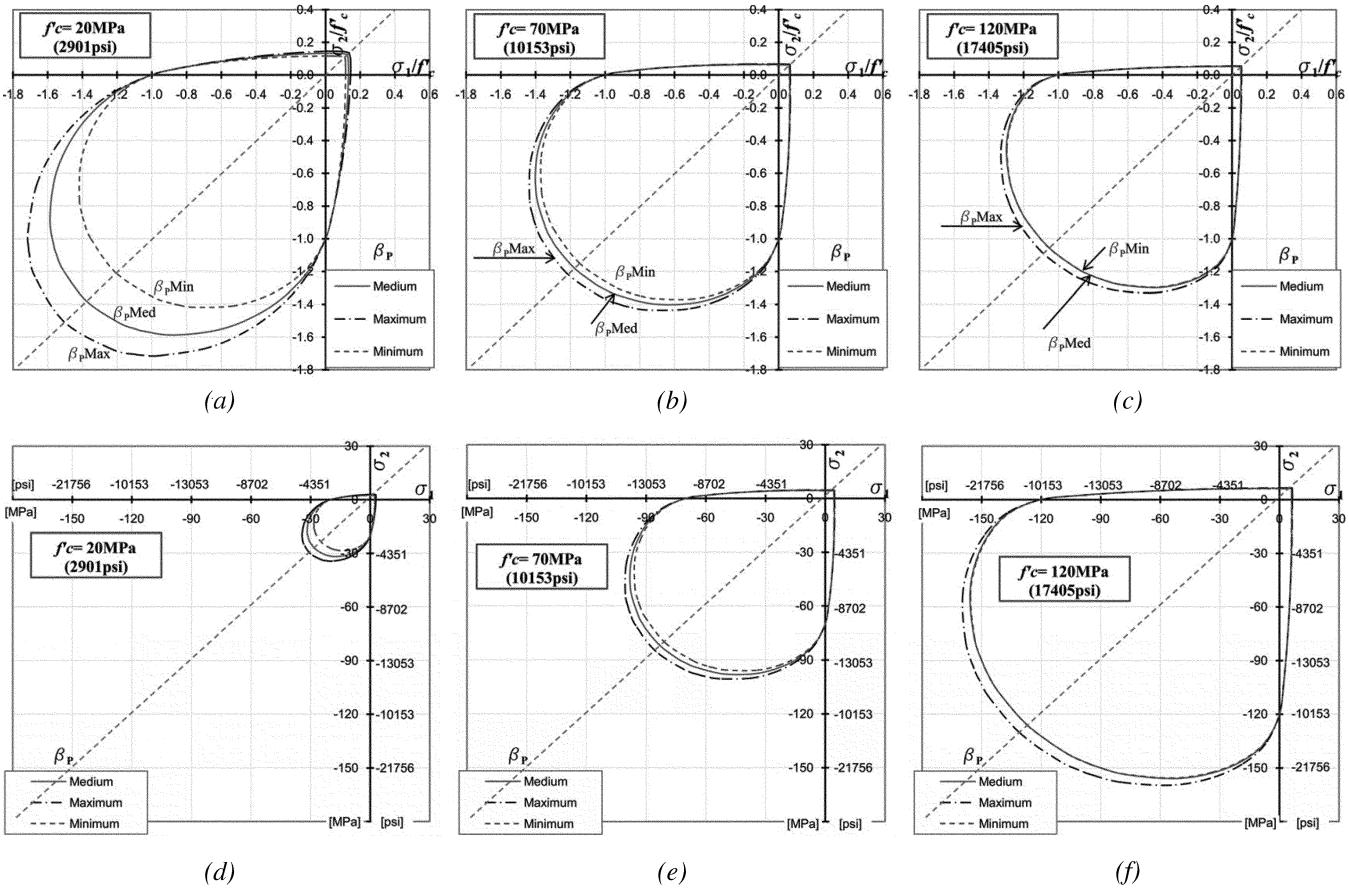

(a) (b) (c)

(d) (e) (f)

Fig. 6—Biaxial failure curves predicted for different β_P *values: (a) normalized curves for* f_c' *= 20 MPa (2901 psi); (b) normalized curves for* f_c' *= 70 MPa (10,153 psi); (c) normalized curves for* f_c' *= 120 MPa (17,405 psi); (d) non-normalized curves for* f_c' *= 20 MPa (2901 psi); (e) non-normalized curves for* f_c' *= 70 MPa (10,153 psi); and (f) non-normalized curves for* f_c' *= 120 MPa (17,405 psi).*

practically unchanged in the tension-tension and compression-tension regimes. This demonstrates the capability of the PDFC to appropriately capture the nonisotropic evolution of the maximum strength surface with increasing concrete quality.

Figures 6(a) to (f) show the PDFC in the biaxial stress space when the maximum, minimum, and medium values of β_P are considered for each selected f_c'. The maximum and minimum values of β_P are determined by Eq. (13) and (14). Comparing the plots in Fig. 5(a) and (b) and Fig. 6(a) to (f), the following conclusions arise:

- The normalized biaxial tensile and, particularly, compressive α_b strengths increase when f_c' decreases. Consequently, NSC is characterized by greater normalized biaxial compressive strength α_b than HSC. When non-normalized plots are considered, however, the biaxial

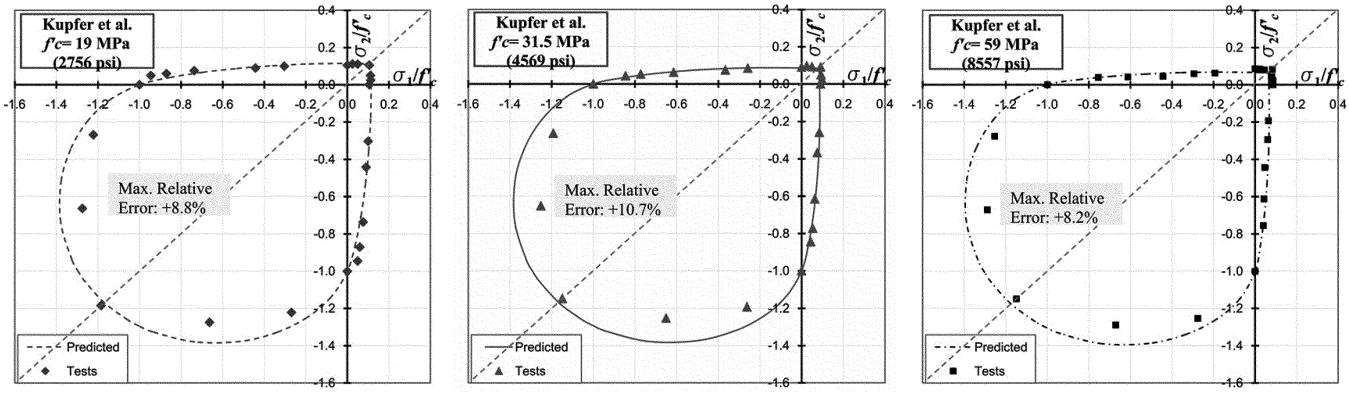

(a) (b) (c)

Fig. 7—Criterion predictions versus Kupfer et al.[8] data: (a) f_c' = 19 MPa (2756 psi); (b) f_c' = 32 MPa (4569 psi); and (c) f_c' = 59 MPa (8557 psi).

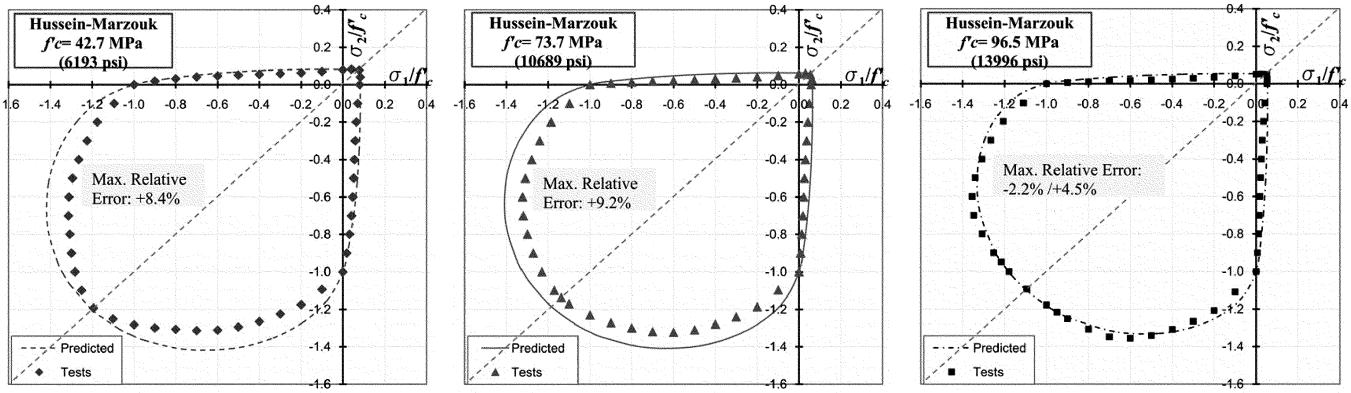

(a) (b) (c)

Fig. 8—Criterion predictions versus Hussein and Marzouk[9] data: (a) f_c' = 43 MPa (6193 psi); (b) f_c' = 74 MPa (10,689 psi); and (c) f_c' = 97 MPa (13,996 psi).

strengths of HSC (in the compressive-compressive regime) are larger than those corresponding to NSC.
- The variation range of the biaxial strength in the compressive-compressive regime in the case of NSC is greater than that corresponding to HSC.
- Concrete quality improvements through increments of f_c' and/or β_P lead to curvature reductions in the maximum strength plots in the biaxial compressive regime. This is valid for both NSC and HSC.

NUMERICAL VALIDATION OF PDFC PREDICTIONS OF CONCRETE MAXIMUM STRENGTHS

With the purpose of validating the PDFC for biaxial and triaxial stress states, several experimental test data were extracted from the literature and compared with the predicted strengths.

The biaxial strength experimental data in this paper were extracted from the following:
- Kupfer et al.[8]: Concrete specimens 200 x 200 x 50 mm (8 x 8 x 2 in.);
- Hussein and Marzouk[9]: Concrete specimens 150 x 150 x 40 mm (6 x 6 x 1.6 in.);
- Lee et al.[10]: Concrete specimens 200 x 200 x 60 mm (8 x 8 x 2.4 in.);
- Lim and Nawy[11]: Concrete specimens 100 x 100 x 100 mm (4 x 4 x 4 in.);
- Ren et al.[12]: Concrete specimens 150 x 150 x 50 mm (6 x 6 x 2 in.); and
- Hampel[13]: Concrete specimens 100 x 100 x 100 mm (4 x 4 x 4 in.).

These tests include both NSC and HSC. Although the specimen geometry, concrete age, and humidity conditions when experiments were performed do not agree in the considered tests, all of them were performed using similar boundary conditions. The PDFC is valid for normalweight concretes and, therefore, lightweight concretes are not included in this predictive analysis.

The comparisons between predicted and experimentally obtained failure strengths are presented in Fig. 7(a) to 11(c). It should be noted that in these numerical evaluations, f_c' represents the mean uniaxial compressive strength of a specimen of the same geometry and age as the ones tested under biaxial loading.

The maximum relative errors of the PDFC predictions are also indicated in these figures. Relative error is evaluated as: error = (predicted value – test result)/test result.

For each set of data, the following procedure was followed:

1. The value of f_c' was extracted as datum from the source paper.

2. (a) If the mixture proportion was explicitly detailed in the paper, the *w/b* was determined, and then the performance parameter was evaluated by Eq. (12); and (b) if the *w/b* was unknown, then the performance parameter was estimated as the mean value of the range of possible β_P defined by Eq. (13) and (14).

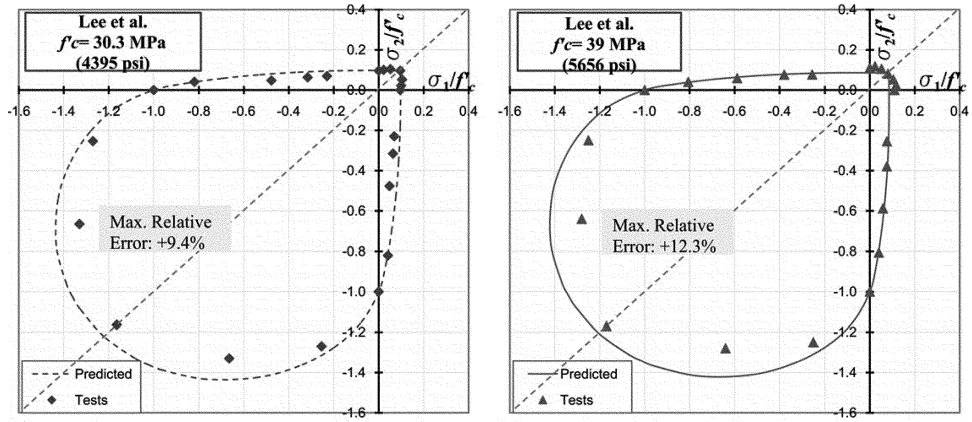

(a) *(b)*

Fig. 9—Criterion predictions versus Lee et al.[10] data: (a) f_c' = 30 MPa (4395 psi); and (b) f_c' = 39 MPa (5656 psi).

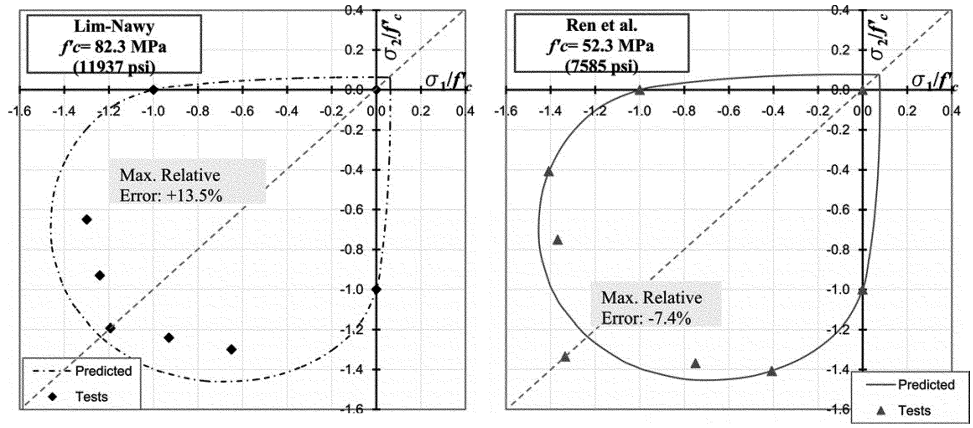

(a) *(b)*

Fig. 10—(a) Criterion predictions versus Lim and Nawy[11] data (f_c' = 82 MPa [11,937 psi]); and (b) criterion predictions versus Ren et al.[12] data (f_c' = 52 MPa [7585 psi]).

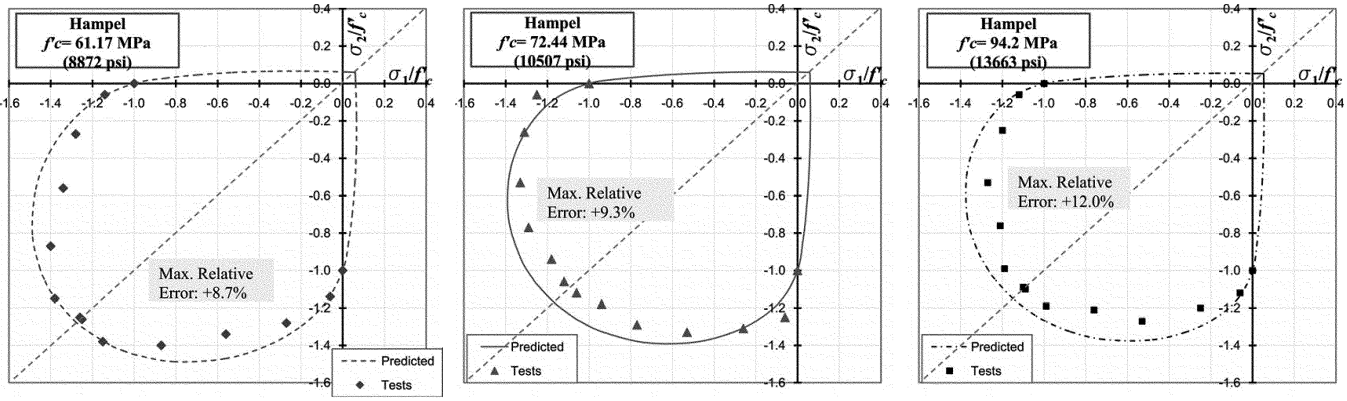

(a) *(b)* *(c)*

Fig. 11—Criterion predictions versus Hampel[13] data: (a) f_c' = 62 MPa (8872 psi); (b) f_c' = 72 MPa (10,507 psi); and (c) f_c' = 94 MPa (13,663 psi).

3. The coefficients A, B_c, B_t, and C were evaluated through Eq. (8) to (11).

No extra calibration was performed for these analyses and comparisons.

The following conclusions arise from the plots in Fig. 7(a) to 11(c), which include 13 sets of data corresponding to concretes in a range of uniaxial compressive strength varying from 19 to 96.5 MPa (2756 to 13,996 psi).

- Good agreement between the predicted and experimentally obtained concrete peak stresses may be observed for the tension-tension quadrant, both for NSC and HSC.
- Good agreement between the predicted and experimentally obtained concrete peak stresses may be observed for the tension-compression quadrants, both for NSC and HSC.
- The maximum relative error varied from 2.2 to 13.5%.

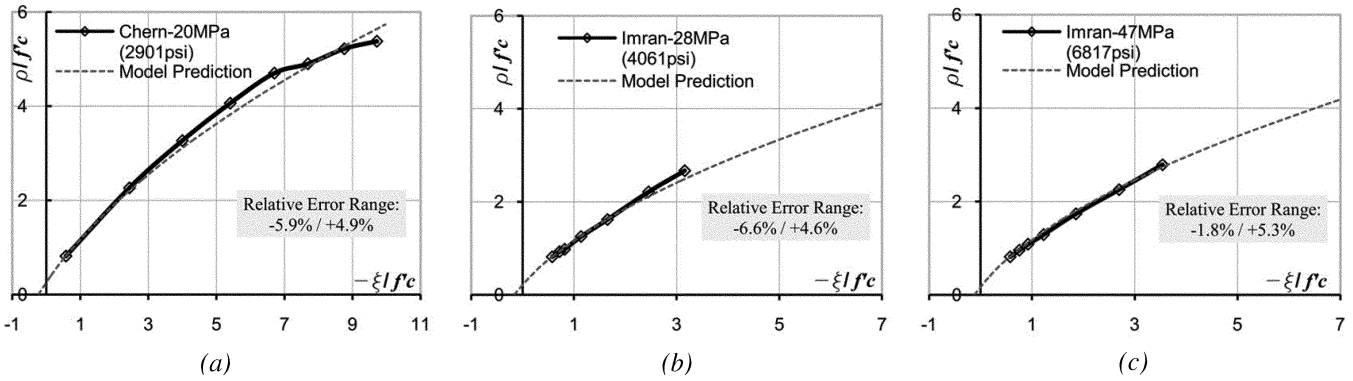

Fig. 12—Validation for triaxial test results: (a) Chern et al.[14] data f_c' = 20 MPa (2901 psi); (b) Imran and Pantazopoulou[15] data f_c' = 28 MPa (4061 psi); and (c) Imran and Pantazopoulou[15] data f_c' = 47 MPa (6817 psi).

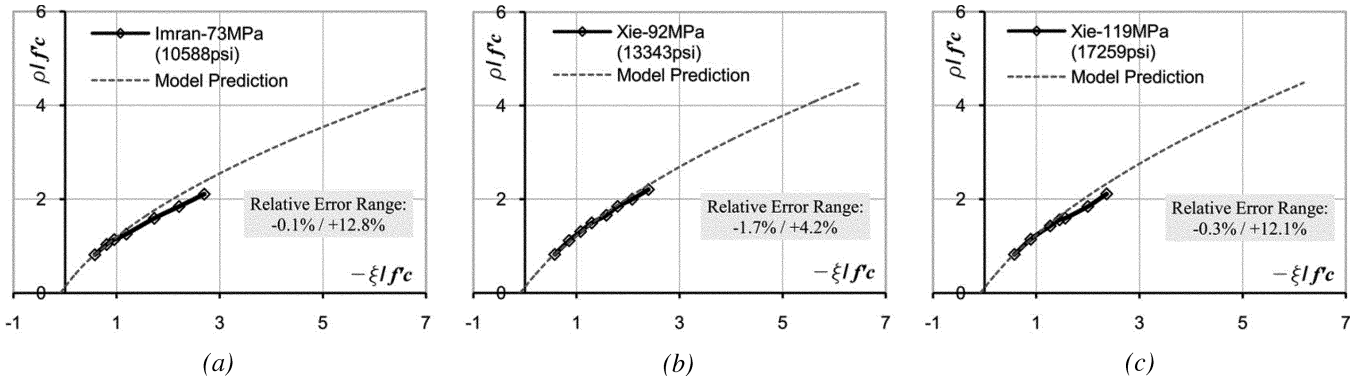

Fig. 13—Validation for triaxial test results: (a) Imran and Pantazopoulou[15] data f_c' = 73 MPa (10,588 psi); (b) Xie et al.[4] data f_c' = 92 MPa (13,343 psi); and (c) Xie et al.[4] data f_c' = 119 MPa (17,259 psi).

- Maximum relative errors are always obtained, both in the case of NSC and HSC, in the compression-compression quadrant. In this sense, it can be observed from the results in Fig. 7(a) to 11(c) that PDFC predictions of peak stresses in this quadrant always overestimate the experimental results. This is partially the consequence of the smooth C1-continuity of the maximum strength surface of the PDFC in the biaxial stress space. In other words, the transition under the C1-continuity condition of the maximum strength curve from the tensile-compression quadrant and, moreover, from the first portion of the compression-compression quadrant (that is, limited by the ratio $\sigma_1/\sigma_2 = 0.25$) to the central portion of this quadrant ($0.25 < \sigma_1/\sigma_2 < 0.75$), necessarily leads to overestimations that vary between 2 and 13% of the maximum strength. Nevertheless, taking into account the large spectrum of considered experiments, performed under different conditions and involving different performances, the very high accuracy obtained in other regions of the biaxial stress space, the considerable advantage of the C1-continuity of the maximum strength surface for numerical implementations of the PDFC, and the involved simplicity of this failure criterion for concretes of arbitrary performance, the overall accuracy of the obtained predictions in the case of biaxial stress states can be considered as very promising.

The PDFC predictions of maximum strengths corresponding to the triaxial experiments are presented in Fig. 12(a), (b), (c) and Fig. 13(a), (b), and (c). Triaxial strength experimental data were extracted from Chern et al.,[14] Imran and Pantazopoulou,[15] and Xie et al.[4]

In general, the accuracy of the maximum strength prediction varies between 0.1 and 12%. Very good agreements with the experimental results are obtained in the low confinement regime; however, it can be clearly recognized from the indicated figures that the relative error increases (as well as the level of overestimation of the experimental strengths) with the confinement level of the involved stress state. As indicated previously, this is a consequence of the C1-continuity condition imposed on the maximum strength parabola of the PDFC while having maximum accuracy in the uniaxial compression condition (low confinement regime).

CONCLUSIONS

In this paper, the internal functions of the PDFC by Folino et al.[7] are reformulated based on an extensive experimental database. Then, PDFC predictive capabilities of experimentally obtained maximum strengths of concretes of arbitrary performances subjected to both biaxial and triaxial stress histories are analyzed. These involve stress states located in all different quadrants of the biaxial stress diagram as well as low and high confinement regions of triaxial stress states.

The PDFC criterion covers the entire spectrum of concrete quality from NSC to HSC. It is represented by two quadratic parabolas for the compressive and tensile meridians with a common vertex on the hydrostatic axis in the stress space expressed in terms of the Haigh Westergaard coordinates. The dependence of the strength criterion on the Lode angle θ follows the elliptical interpolation by Willam and Warnke.[3]

The input data are reduced to only two material parameters: the uniaxial compressive strength and the so-called concrete performance parameter.

The conclusions drawn from this paper may be summarized as follows:

- The strengths predicted by the PDFC for biaxial stress states located in the compression-compression, compression-tension, and tension-tension quadrants show good agreement with the experimentally obtained peak stresses in the biaxial tensile, tensile-compression, and low level of the compressive-compressive quadrants.
- The accuracy of the PDFC decreases to approximately 87 to 96% in the zone of the biaxial compressive-compressive quadrant limited by $0.25 < \sigma_1/\sigma_2 < 0.75$.
- In the case of triaxial stress histories, the accuracy of the PDFC predictions decreases to 88 to 95% when the stress states activate very high confining pressures.
- The convexity condition included in the PDFC imposes constraints between three of the material features regarding quality—that is, the uniaxial tensile strength ratio α_t, the biaxial compressive strength ratio α_b, and the tangent m to the compressive meridian on the peak stress's shear component corresponding to the uniaxial compression test.
- The criterion correctly reproduces the nonisotropic changes in the concrete peak strength surface that take place when increasing material quality is considered (increasing uniaxial compressive strength property).
- The performance parameter takes into account the influence of the particular concrete mixture on the maximum strength surface.
- Therefore, the criterion permits the prediction of the entire range of failure surfaces corresponding to a given f_c' and different concrete mixtures.

The proposed criterion is being implemented as the maximum strength surface in an inelastic constitutive model for concretes,[16] which consequently also depends on the concrete performance.

ACKNOWLEDGMENTS

The authors gratefully acknowledge the partial financial support of this work by the ANPCyT—Argentina (Project PICT 2006-01232), the University of Buenos Aires (UBACYT 2006-2009 Project I813), and the INTECIN and the Laboratory of Materials and Structures at the University of Buenos Aires.

REFERENCES

1. Drucker, D., and Prager, W., "Soil Mechanics and Plastic Analysis or Limit Design," *Quarterly of Applied Mathematics*, V. 10, 1952, pp. 157-165.

2. Ottosen, N., "A Failure Criterion for Concrete," *Journal of Engineering Mechanics Division*, ASCE, V. 103, No. 4, 1977, pp. 527-535.

3. Willam, K. J., and Warnke, E. P., "Constitutive Model for the Triaxial Behavior of Concrete," Proceedings of the International Association for Bridge and Structural Engineering, *Report* 19, Section III, Zurich, Switzerland, 1974, pp. 1-30.

4. Xie, J.; Elwi, A.; and MacGregor, J., "Mechanical Properties of Three High-Strength Concretes Containing Silica Fume," *ACI Materials Journal*, V. 92, No. 2, Mar.-Apr. 1995, pp. 135-145.

5. Ansari, Q., and Li, Q., "High-Strength Concrete Subjected to Triaxial Compression," *ACI Materials Journal*, V. 95, No. 6, Nov.-Dec. 1998, pp. 747-755.

6. Seow, P., and Swaddiwudhipong, S., "Failure Surface for Concrete under Multiaxial Load—A Unified Approach," *Journal of Materials in Civil Engineering*, ASCE, V. 17, No. 2, 2005, pp. 219-228.

7. Folino, P.; Etse, G.; and Will, A., "A Performance Dependent Failure Criterion for Normal and High Strength Concretes," *Journal of Engineering Mechanics*, ASCE, V. 135, No. 12, 2009, pp. 1393-1409.

8. Kupfer, H.; Hilsdorf, H.; and Rusch, H., "Behavior of Concrete under Biaxial Stresses," ACI JOURNAL, *Proceedings* V. 66, No. 8, Aug. 1969, pp. 656-666.

9. Hussein, A., and Marzouk, H., "Behavior of High-Strength Concrete under Biaxial Stresses," *ACI Materials Journal*, V. 97, No. 1, Jan.-Feb. 2000, pp. 27-36.

10. Lee, S.; Song, Y.; and Han, S., "Biaxial Behavior of Plain Concrete of Nuclear Containment Building," *Nuclear Engineering and Design*, V. 227, 2004, pp. 143-153.

11. Lim, D., and Nawy, E., "Behavior of Plain and Steel-Fiber-Reinforced High Strength Concrete under Uniaxial and Biaxial Compression," *Magazine of Concrete Research*, V. 57, No. 10, 2005, pp. 603-610.

12. Ren, X.; Yang, W.; Zhou, Y.; and Li, J., "Behavior of High-Performance Concrete under Uniaxial and Biaxial Loading," *ACI Materials Journal*, V. 105, No. 6, Nov.-Dec. 2008, pp. 548-557.

13. Hampel, T., "Experimental Analysis of the Behavior of High Performance Concrete under Multiaxial States of Stresses," PhD thesis, Technischen Universität Dresden, Dresden, Germany, 2006.

14. Chern, J.; Yang, H.; and Chen, H., "Behavior of Steel Fiber Reinforced Concrete in Multiaxial Loading," *ACI Materials Journal*, V. 89, No. 1, Jan.-Feb. 1992, pp. 32-40.

15. Imran, I., and Pantazopoulou, S. J., "Experimental Study of Plain Concrete under Triaxial Stress," *ACI Materials Journal*, V. 93, No. 6, Nov.-Dec. 1996, pp. 589-601.

16. Etse, G., and Folino, P., "Elastoplastic Constitutive Model for Concretes of Arbitrary Strength Properties," *Proceedings of Euro-C 2010*, Rohrmoos, Schladming, Austria, 15-18 March 2010, *Computational Modelling of Concrete Structures*, N. Bicanic, R. de Borst, H. Mang, and G. Meschke, eds., CRC Press, Taylor and Francis Group, London, UK, 2010, pp. 129-135.